Understanding Sterol-Membrane Interactions, Part II: Complete ^{1}H and ^{13}C Assignments by Solid-State NMR Spectroscopy and Determination of the Hydrogen-Bonding Partners of Cholesterol in a Lipid Bilayer**

Olivier Soubias,[a] Franck Jolibois,[b] Valérie Réat,[a] and Alain Milon*[a]

Abstract: The complete assignment of cholesterol ^{1}H and ^{13}C NMR resonances in a lipid bilayer environment (L_{α}-dimyristoylphosphatidylcholine/cholesterol 2:1) has been obtained by a combination of 1D and 2D MAS NMR experiments: ^{13}C spectral editing, ge-HSQC, dipolar HETCOR and J-based HETCOR. Specific chemical shift variations have been observed for the C1–C6 atoms of cholesterol measured in CCl_4 solution and in the membrane. Based on previous work (F. Jolibois, O. Soubias, V. Réat, A. Milon, *Chem. Eur. J.* **2004**, *10*, preceding paper in this issue: DOI: 10.1002/chem.200400245) these variations were attributed to local changes around the cholesterol hydroxy group, such as the three major rotameric states of the C3–O3 bond and different hydrogen bonding partners (water molecules, carboxy and phosphodiester groups of phosphatidylcholine). Comparison of the experimental and theoretical chemical shifts obtained from quantum-chemistry calculations of various transient molecular complexes has allowed the distributions of hydrogen bonding partners and hydroxy rotameric states to be determined. This is the first time that the probability of hydrogen bonding occurring between cholesterol's hydroxy group and phosphatidylcholine's phosphodiester has been determined experimentally.

Keywords: ab initio calculations · hydrogen bonds · NMR spectroscopy · steroids · sterol-membrane interactions

Introduction

Cholesterol is an important constituent of animal cell membranes in which it accounts for up to 50 mol% of the membrane lipids. The biological roles of cholesterol involve the maintenance of proper fluidity, the formation of glycosphingolipid cholesterol-enriched domains, the reduction of passive permeability and increased mechanical strength of the membrane.[2–4] Because cholesterol plays such an important role in the membrane, phospholipid–cholesterol interactions have been studied extensively. Owing to its amphiphilic properties, cholesterol is oriented within a lipid bilayer with its long axis normal to the membrane surface. The pseudorigid four-fused-ring skeleton interacts with the phospholipid's acyl chains to optimize hydrophobic interactions and the polar hydroxy group points towards the bilayer surface. Nonpolar interactions between the sterol ring and the phospholipid chains are not easy to investigate. Some experimental[5] and molecular modelling[6] studies have shown that ring–chain interactions are less favored than chain–chain interactions. There have been many suggestions that hydrogen bonds form between cholesterol and certain atoms of the phosphatidylcholine (PC) polar head.[7–10] For instance, molecular dynamics simulations have allowed the interactions between phospholipids, cholesterol and water to be examined in detail.[6,11–15] These studies have shown that the cholesterol's hydroxy group can interact strongly with water and carbonyl and phosphate oxygen atoms of phosphatidylcholine. But so far there have been very limited experimental data to support these conclusions. The use of X-ray and neutron diffraction and proton-deuterium contrast methods as well as molecular dynamics calculations has demonstrated that cholesterol is well embedded in the membrane and occupies a vertical location that favors a hydrogen-bonding interaction between its OH group and the phospholipid's fatty acyl chain esters.[16–22] By using FTIR spectroscopy to study anhydrous lipid mixtures, Wong et al. have demonstrated that hydrogen bonding occurs between the cholesterol's OH group and the lipid's sn-2 chain carbonyl and phosphate groups.[9] However, no evidence of hydrogen bonding between cholesterol and the carbonyl groups at the diester

[a] Dr. O. Soubias, Dr. V. Réat, Prof. Dr. A. Milon
Institut de Pharmacologie et de Biologie Structurale,
CNRS and University P. Sabatier
205 rte de Narbonne, Toulouse (France)
Fax: (+33) 561-175-424
E-mail: alain.milon@ipbs.fr

[b] Dr. F. Jolibois
Laboratoire de Physique Quantique, UMR 5626, IRSAMC
University P. Sabatier
118 rte de Narbonne, Toulouse (France)

[**] For Part I see ref. [1].

 DOI: 10.1002/chem.200400246

linkages of the PC lipids was found in independent studies using Raman[23] and infrared spectroscopy[24] and studies of membrane permeability[25] with a PC membrane in the presence or absence of cholesterol. The replacement of one or both of the acyl groups of phosphatidylcholine with alkyl groups (i.e. an ether linkage instead of an ester linkage) enhanced the interaction with cholesterol, which further indicates the importance of the interfacial region in the interaction.[26] The results of earlier studies indicated that a hydrogen bond exists between the hydroxy group of cholesterol and the phosphate headgroup of a phospholipid.[27] However, the presence of such a hydrogen bond was refuted by subsequent ^{13}C and ^{31}P NMR spectroscopic studies.[28] Therefore, the molecular basis of the cholesterol–phosphatidylcholine association has not been unequivocally established.[4,29]

Solid-state NMR spectroscopy is a powerful tool with which to study membrane molecule interactions because it allows the direct study of amorphous and partly mobile biological solids in the liquid-crystalline lipid bilayer. Currently, most of solid-state NMR experiments on phospholipid/cholesterol systems have been focused on the phospholipid component or on the dynamics of cholesterol.[25,30–35] However, chemical shifts are intimately related to the local environment around the nuclei and could reveal the nature of lipid–cholesterol interactions. In recent work, we have shown that the chemical shifts calculated by quantum-chemical methods could be used to reproduce experimental solution-state chemical shifts, both in the presence and in the absence of hydrogen bonds, with a satisfactory degree of accuracy.[1] However, the assignment of cholesterol NMR resonances in a membrane medium remains a difficult task since standard liquid-state NMR procedures cannot be applied in such liquid-crystalline media. In this paper, we present the complete and unambiguous ^{1}H and ^{13}C assignment of cholesterol in L_{α}-dimyristoylphosphatidylcholine (DMPC) membranes based on a combination of 1D MAS ^{13}C NMR spectra with various polarization transfer schemes and 2D MAS ^{1}H–^{13}C, ge-HSQC and dipolar HETCOR experiments. A comparison of the carbon chemical shifts of cholesterol in solution and in its membrane environment revealed distinct differences in the first two rings, that is, in atoms C1–C6. These variations have been interpreted in terms of hydrogen bonding and rotameric states of the hydroxy group by comparing experimental chemical shift variations with those obtained from quantum-chemical calculations. We show that experimental chemical-shift restraints can be used to probe the local environment of the cholesterol hydroxy group in a membrane and to quantify the distribution of its hydrogen bonding partners.

Results and Discussion

Assignment strategy of cholesterol in membranes: The assignment strategy for the NMR resonances of sterols is well established as long as they are in solution and the rapid tumbling of molecules averages out the anisotropic interactions such as chemical shift anisotropy and dipole–dipole interactions. Heteronuclear 2D experiments, such as HMQC, provide one-bond connectivity information, which correlate directly bound carbon and hydrogen atoms. 2D experiments, such as HMBC, permit sequential assignment by connecting H and C atoms separated by two or three bonds. Homonuclear COSY and NOESY experiments provide proton–proton connectivity and stereospecific assignments.[36] Nevertheless, the complete assignment of sterols in their natural lipid environment remains a difficult task. For small- to medium-sized compounds in a liquid-crystalline phase, magic angle spinning (MAS) and high-power proton decoupling yield rather well resolved and sensitive one-dimensional NMR spectra of low γ nuclei such as ^{13}C in a routine fashion. In analogy to the liquid-state case, several spectral editing techniques, which separate ^{13}C resonances according to their multiplicities, have been proposed and used to characterize the ^{13}C NMR spectra of organic molecules.[37–40] The transfer through J coupling provides well resolved and selective chemical-shift correlation between directly bound proton–carbon pairs, provided that the coherences involved decay more slowly than the delay required for efficient polarization transfer.[41,42] For the particular case of sterols in membranes, we have recently used the gain in sensitivity brought about by inverse detection to detect all the expected one-bond cross peaks of natural abundance cholesterol in a DMPC/cholesterol lipid mixture.[43] However, fast relaxation processes have so far prevented long-range J-coupling-based experiments and the observation of multiple-bond connectivity. Furthermore, for reasons of sensitivity, ^{13}C–^{13}C homonuclear correlation techniques[44–46] are rarely applicable to natural abundance materials in membrane samples. One way to recover skeletal information is to transfer magnetization through dipolar coupling to obtain through-space correlation, that is, cross peaks between bound and non-bound pairs. Herein , we have thus used a combination of one-dimensional (1D) and two-dimensional (2D, HSQC and dipolar HETCOR) MAS solid-state NMR techniques to perform the complete, stereospecific, ^{1}H and ^{13}C assignment of natural abundance cholesterol in a membrane without any reference to the known liquid-state assignment (Table 1; Scheme 1).

One-bond (^{1}H–^{13}C) correlations from HSQC experiments: As discussed by Soubias et al.,[43] 2D HR-MAS gradient-enhanced HSQC experiments provided all the expected ^{1}H–^{13}C one-bond cross peaks of cholesterol in the membrane state, thus giving the corresponding proton chemical shift for each peak of the one-dimensional carbon spectrum.

Carbon multiplicities: Quaternary carbon atoms were identified by performing a CP-MAS experiment with a long contact time. ^{13}C multiplicity-edited spectra were obtained by varying the second delay (Δ) of a refocused INEPT 1D MAS experiment performed at 9 kHz. The spectra with $\Delta = 1/4\,J$, $1/3\,J$ ($^{1}J_{C\text{-}H} = 136$ Hz) were compared with the standard INEPT spectrum. The spectrum obtained with $\Delta = 1/4\,J$ (selection of CH and CH_3) has allowed us to identify the five expected methyl resonances at $\delta = 11.84$, 18.61, 19.14 and 21.89 ppm (C26 and C27 are superimposed). Methine

Table 1. Assignment of carbon and proton chemical shifts for cholesterol inserted in a DMPC/cholesterol 7:3 lipid mixture at 313 ± 2 K.

^{13}C chemical shift [ppm][a]	^{1}H chemical shift [ppm][b]	Carbon multiplicities[c]	Nonbonded contacts[d]	Assignment
11.84	0.67	CH_3	C13	C18
18.61	0.9	CH_3	H20 or H22(1,26)	C21
19.14	0.97	CH_3	C10	C19
20.93	1.46	CH_2	H9/H12(1.96)	C11
21.89	0.71	CH_3	H25	C26/C27
21.89	0.71	CH_3	H25	C26/C27
24.27	1.46	CH_2	H16(1.2—1.8)/H14 + H17	C15
24.53	1.31/1.05	CH_2	H22(1.26)/H26 + H27	C23
27.53	1.4	CH	H24	C25
28.03	1.8 pro*S*/1.2 pro*R*	CH_2	H14 + H17 (1.02)	C16
30.61	1.76(e)/1.45(a)	CH_2	H1(0.98)/H3	C2
32.59/32.65	1.41	CH	H14/H7	C8
32.59/32.65	1.89(e)/1.41(a)	CH_2	H8(1.41)/H6	C7
36.08	–	Q	H2(1.71)/H19	C10
36.13	1.26/0.85	CH_2		C22
36.23	1.26	CH	H21	C20
37.33	1.71(e)/0.98(a)	CH_2	H2(1.45)/H9	C1
39.05	1.03	CH_2	H23	C24
39.77	1.96(e)/1.16(a)	CH_2	H11/H19	C12
41.39	2.22	CH_2	H3/H2	C4
42.05	–	Q	H18	C13
49.99	0.88	CH	H11	C9
56.64	1.04	CH	H20/H16	C14 or C17
56.66	1.02	CH	H20/H16	C14 or C17
70.25	3.37	CH	H2/H4	C3
119.78	5.21	CH	C7	C6
141.73	–	Q	H4	C5

[a] Frequencies in the carbon dimension are given with respect to C18, which was set to $\delta = 11.84$ ppm with respect to TMS by analogy with a liquid-state spectrum recorded in CCl_4 at 313 K. Uncertainty in the reported chemical shifts is estimated to be ±0.02 ppm. [b] Frequencies in the proton dimension are given with respect to H18, which was set to 0.67 ppm with respect to TMS by analogy with a liquid-state spectrum recorded in $CDCl_3$ at 313 K. Stereospecific assignments of methylene protons (a: axial; e: equatorial) were extracted from dipolar HETCOR experiments (contact time 250 μs). Uncertainty in the reported chemical shifts is estimated to be ±0.05 ppm. [c] Identification of the carbon multiplicities was determined by scalar-coupling-based spectral editing and other experiments (see text for details). [d] Contacts between protons and carbons extracted from dipolar HETCOR carbon traces (contact time 2.5 ms).

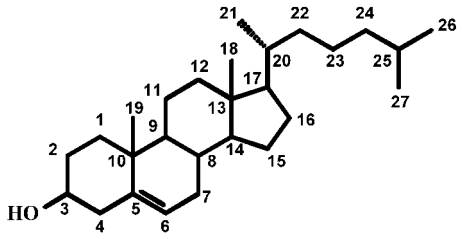

Scheme 1. Structure of cholesterol; classical nomenclature is used.

groups were assigned by comparison of the carbon spectra obtained with $\Delta = 1/4\,J$ and $\Delta = 1/3\,J$ (eight positive resonances). For the methylene groups, a lower signal-to-noise ratio was observed because of the fast transverse relaxation of the tightly coupled methylene protons during the overall INEPT delay. Hence, negative and missing isolated resonances have been assigned to methylene carbon atoms ($\delta = 9/11$, 20.93, 24.27, 24.53, 28.03, 30.61, 37.33, 39.05, 39.77, and 41.39 ppm). One of the remaining methylene carbon atoms was has been assigned by recording a long contact time CP-MAS spectrum with no decoupling during the acquisition. In the region centered around 36.2 ppm, we observed a multiplet with signal intensities close to a 1:1:2s:1:1 ratio (2s refers to a carbon intensity of 2 plus a shoulder), which could be assigned to the superposition of a CH (36.23 ppm), a CH_2 (36.13 ppm) and a quaternary carbon atom (36.08 ppm). The peak centered on 32.5 ppm was assigned to the two remaining resonances, one methane, and one methylene.

Multiple-bond (^{1}H–^{13}C) correlations from dipolar HETCOR experiments: A cross-polarization period transfers magnetization from protons to the neighboring carbon atoms in an oscillatory manner for an isolated two-spin system. The coherence transfer efficiency depends on the geometry and dynamics of the system, that is, on the size of the effective heteronuclear couplings, the CP mixing time and the spin dynamics of CP.[45,47,48] The dynamics of cholesterol in a DMPC membrane can be well described as fast axial diffusion along the bilayer normal with a small amplitude of wobbling ($S_{mol} = 0.92$).[35] This movement converts the homogeneous proton dipolar broadening into an inhomogeneous broadening, which can be effectively averaged out by MAS.[49] At moderate MAS spinning rates, such as the 9 kHz used herein, this movement also transforms the ^{1}H–^{13}C spin pairs into virtually isolated spin pairs. It was checked experimentally that CP and Lee–Goldburg CP[50] magnetization transfer display comparable kinetics in agreement with this assumption (data not shown). Finally, the ^{1}H–^{13}C dipolar couplings of directly bound pairs depend not only on the internuclear distances but also on the internuclear vector orientation with respect to the diffusion axis. This formed the basis for the stereospecific assignment of axial and equatorial methylene protons. Figure 1 shows the simulated cross-polarization transfer efficiency obtained at the first recoupling sideband of the Hartman–Hahn matching curve for isolated spin pairs with various dipolar couplings, calculated according to Lesage et al.[45] We clearly see that for mixing times close to 2.5 ms, the transfer efficiency is similar for protons with dipolar couplings ranging from 1 to 9 kHz. In contrast, a mixing time close to 1 ms leads to a more selective transfer that can be used to distinguish spin systems. Thus, cross-peak intensities and chemical shift dispersion can be used as a guideline when analysing the results of dipolar HETCOR experiments. Both strategies have

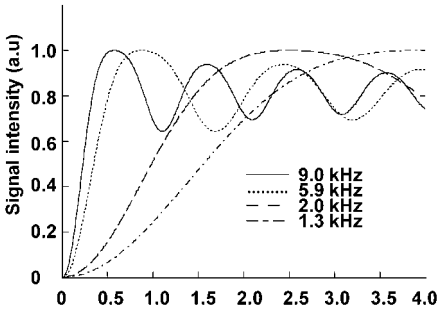

Figure 1. Simulated coherence transfer efficiency as a function of mixing time in a dipolar HETCOR experiment with typical values of heteronuclear dipolar couplings for a DMPC/cholesterol mixture. The calculations were performed according to Lesage et al.[45] Relaxation was not taken into account.

been used and the results can be appreciated in Figure 2 (chemical-shift dispersion) and Figure 3 (spin-system assignment).

Figure 2 serves to illustrate the assignment of cholesterol ring A from a combination of HSQC and dipolar HETCOR experiments. H–C dipolar couplings in cholesterol can be calculated from the known dynamics of cholesterol under the experimental conditions.[35,51] As shown in Figure 2B the only protons to display a significant (>1 kHz) dipolar coupling with C1 are $H1_{a,e}$ and $H2_{a,e}$. Correspondingly, the two HSQC traces in Figure 2A reveal one bond connections between a) C1 and the two H1 protons and b) C2 and the two H2 protons. The dipolar HETCOR trace along C1 contains connections with both H1 and H2 protons, which guides the assignment of C1 to H2 and C2 (Figure 2Ac). It can be observed that as a result of the 2.5 ms contact time the signal intensities are independent of the dipolar couplings in the 1–10 kHz range, in agreement with the simulations shown in Figure 1.

The complete assignment was performed in this way ("HMBC-like" strategy) starting from resonance C3 ($\delta =$ 70.25 ppm), which could be safely assigned from carbon chemical shift considerations and multiplicity. Table 1 shows all the useful correlations in the dipolar HETCOR experiment (column "nonbonded contacts").

In addition to these traces the C15–C16 spin system with the corresponding calculated one-bond and two-bond dipolar couplings is represented in Figure 3 (e.g. H16 proR has a 0.1 kHz one-bond dipolar coupling with C16 and a 2.3 kHz two-bond dipolar coupling with C15).

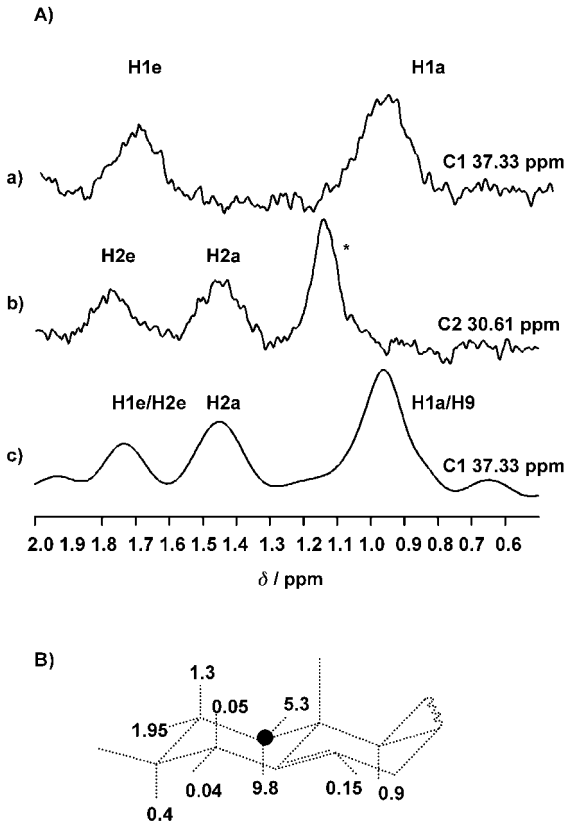

Figure 2. Combination of ge-HSQC and dipolar HETCOR for the assignment of NMR resonances of cholesterol. A) Cross sections along the proton dimension at carbon chemical shifts corresponding to C1 (a,c) and C2 (b) extracted from ge-HSQC (a,b) and dipolar HETCOR (2.5 ms contact time) (c). Comparison of the cross sections and favorable chemical shift dispersion allows the assignment of C1. * This signal arises from natural abundance lipid methylene. B) Dipolar couplings between C1 and neighboring protons (in kHz) calculated from the known structure and dynamics of cholesterol.[35]

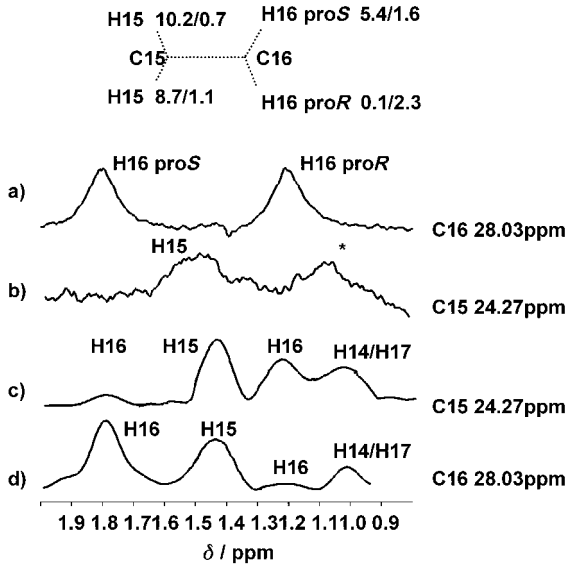

Figure 3. Assignment of the C15–C16 spin system. a) Carbon slice extracted from the HSQC experiment at 28.03 ppm. b) Carbon slice extracted from the HSQC experiment at 24.27 ppm. c) Carbon slice extracted from the dipolar HETCOR experiment at $\delta = 24.27$ ppm with a mixing time of 0.8 ms. d) Carbon slice extracted from the dipolar HETCOR experiment at $\delta = 28.03$ ppm with a mixing time of 2 ms.

The use of a shorter CP mixing time is illustrated for the C15–C16 spin system. Figure 3 shows carbon slices extracted from the HSQC experiment at a) 28.03 and b) 24.27 ppm and from the dipolar HETCOR experiment at c) 24.27 ppm with a mixing time of 0.8 ms, and d) at 28.03 ppm with a mixing time of 2 ms (d). One- and two-bond calculated H–C dipolar couplings are also indicated. H16 proR has a very

weak one-bond dipolar coupling with C16 (0.1 kHz) because this internuclear vector is almost at the magic angle with the molecular diffusion axis. This characteristic was unique in the molecule and contributed to the assignment of the C16 spin system. Accordingly a very small cross peak is observed between C16 and H16 proR in Figure 3d, while the HSQC experiment clearly shows that the two protons, H16 proR and H16 proS, are not equivalent (Figure 3a). At this mixing time of 2 ms, the two-bond dipolar couplings of about 1 kHz for both H15 protons give rise to a strong cross peak between C16 and H15. At a shorter mixing time of 0.8 ms (Figure 3c) a distinction is made between C15–H16 proS (1.6 kHz dipolar coupling) and C15–H16 proR (2.3 kHz dipolar coupling) that results in a stronger cross peak. This analysis permitted both sequential and stereospecific assignments of this particular spin system.

The difference between axial and equatorial protons is even stronger at shorter mixing times. Figure 4 shows that the two methylene protons can be readily distinguished in the dipolar HETCOR experiment at 0.25 ms in the case of C12 (dipolar coupling of 2 kHz for H12e and 10.3 kHz for H12a; the ratio of the two cross-peak intensities is 9), as shown both theoretically (Figure 4A) and experimentally (Figure 4B). This approach was also applied to the stereospecific assignment of H1, H2, and H7 methylene protons.

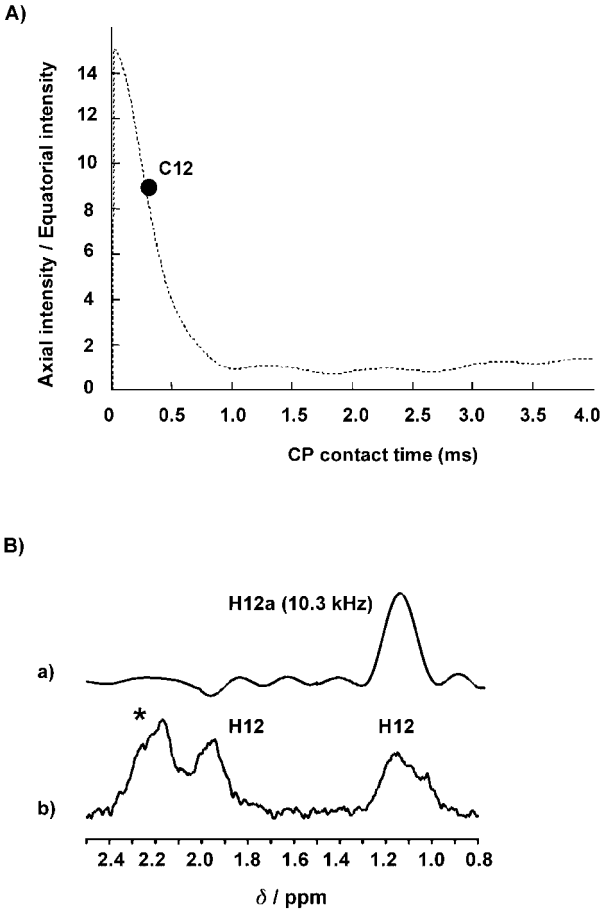

Figure 4. A) Evolution of the ratio (axial versus equatorial) of the transfer efficiency between diastereotopic protons with the mixing time (calculated as in ref. [45]). For a mixing time of 250 μs, the selectivity of transfer is predicted to be equal to 9 for C12. B) Carbon slices extracted at $\delta = 39.77$ ppm (corresponding to C12) from the dipolar HETCOR experiment with a mixing time of 250 μs (a) and the HSQC experiment (b). The two H12 protons ($\delta = 1.16$, 1.96 ppm) can be easily identified in the HSQC experiment. The same carbon slice extracted from the dipolar HETCOR experiment shows only one cross peak at $\delta = 1.16$ ppm, which corresponds to the axial H12 hydrogen. *This signal arises from natural abundance lipids (side-chain methylene C2).

As summarized in Table 1 we could thus perform the complete, stereospecific assignment of all carbon and proton resonances of cholesterol, without any reference to the liquid-state assignment. As will be discussed below, this is particularly important since we have observed significant differences between the chemical shifts of cholesterol in solution and in membrane, up to 1.5 ppm, whereas for instance C4 chemical shift differs only from C12 and C13 by 1.6 and 0.7 ppm, respectively. It is clear from the above discussion that our strategy can only be extended to fast, axially diffusing, rigid membrane components of known dynamics and orientation, such as cholesterol, since it largely relies on the quantitative analyses of heteronuclear dipolar couplings.

Cholesterol–phosphatidylcholine interactions—probing hydrogen-bonding effects with quantum chemical calculations and ^{13}C NMR carbon chemical shift variation patterns: The current knowledge of interactions between cholesterol and phosphatidylcholines or interfacial water is still incomplete even though it has been extensively studied in a variety of membrane models and by a large number of biophysical approaches (for a recent review, see the publication by Ohvo-Rekila et al.[4]) It is customary to assume that the hydroxy group of cholesterol resides in the interfacial region of the bilayer where it forms transient hydrogen bonds.[7–10,52] Interactions with the available hydrogen-bonding partners, that is, fatty acid ester bonds, phosphodiesters and water molecules, have been observed in molecular dynamics simulations.[11–15] NMR spectroscopy has been used to analyse the chemical shift variation of fatty acid carbonyl groups between a pure DMPC sample and a DMPC/cholesterol mixture. The results qualitatively indicate that the interactions between lipids and cholesterol occur through the DMPC carbonyl group.[53] However, to our knowledge, there are very limited experimental data to support the conclusions provided by molecular dynamics simulations and the formation of direct hydrogen bonds between PC and cholesterol in the PC/Cholesterol membrane has been a controversial issue over the years.[4,54] It has long been known that conformational effects (including dihedral angles and the type of neighboring atoms), hydrogen bonding or the chemical nature of the solvent influences the NMR chemical shifts. Therefore, it should be interesting to analyze the spectroscopic response of cholesterol to interactions with its environment on the basis of the new carbon and proton chemical shift information.

Chemical shift variation pattern from NMR data: The following analysis assumes that no major structural change in cholesterol occurs upon dilution in carbon tetrachloride (CCl_4) and DMPC membranes. This hypothesis seems reasonable in the case of the "rigid part" of the molecule (C1–C16). It

is certainly not valid for the side chain, for which the conformational equilibria are sensitive to packing effects in the lipid bilayer, so these chemical shifts will not be discussed further.

Chemical shift variations between cholesterol in anhydrous CCl_4 and the DMPC membrane reflect the influence of the surrounding medium. This can be broken down into a "general solvent effect", uniformly distributed over the sterol structure, and into more specific interactions at the hydroxy group, such as hydrogen bonds and the unequal distribution of rotamers around the C3–O3 bond. As shown in our previous work,[1] hydrogen bonding and the preferential conformation of the hydroxy group are expected to affect mainly the chemical shifts of the carbon atoms located in the first two rings.

Absolute chemical shifts are difficult to define in the case of heterogeneous systems, such as the membrane/water system, since an "internal reference", such as TMS, partitions between the two phases and has a different resonance frequency in each phase.[55] Therefore, no TMS was added, and in Table 1 chemical shifts are referenced with respect to the resonance of methyl-18 (relative to TMS) by analogy with a liquid-state spectrum recorded in CCl_4. By doing so, we observed that all the carbon chemical shifts of rings B, C, and D (C7–C16) were identical to within ± 0.15 ppm in solution and in membranes. To calculate the chemical shift variations for C1–C6 for cholesterol in CCl_4 solution and in membranes, we subtracted the average chemical shift variation of C8, C9 and C11–C16. *It should be stressed that, by doing so, the results do not depend on the choice of C18 as a chemical shift reference*. The chemical shift variation pattern obtained for all cholesterol carbons when this nonspecific "solvent effect" is subtracted is shown in Figure 5. Therefore, the magnitude and sign of the variation reveal the extent of the hydrogen-bonding effect and/or the unequal distribution between the rotameric states of the 3β-OH for C1–C6. The observed variations for C17, C20–C23 probably reflect a different conformation of the side chain. A positive value for the chemical shift variation corresponds to a downfield shift (deshielding) in the membrane relative to the liquid state. C2–C4 and C6 show negative variations with values ranging from −0.86 ppm (C3) to −1.5 ppm (C6); C1 has a variation close to 0 and C5 is deshielded by around 1.2 ppm.

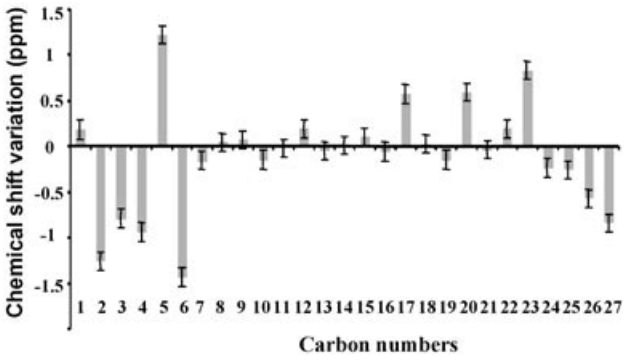

Figure 5. Experimental chemical shift variation pattern between cholesterol in the DMPC membrane and in CCl_4 solution ($\Delta\delta_i^{exp} = [\delta_i^{exp}(\text{membrane}) - \delta_i^{exp}(CCl_4)]$).

Quantum-chemical calculation of the chemical shift variation pattern induced by hydrogen bonding: We have recently shown that the experimental effect of hydrogen-bonding on chemical shifts can be efficiently calculated by using a quantum-chemical approach.[1]

In an attempt to mimic the sterol environment (solvent and lipids), several hydrogen-bond partners for the cholesterol's hydroxy group were considered, that is, water molecules, the acyl chain's ester bonds, and the lipid's phosphodiesters. Water molecules can be hydrogen-bond donors or acceptors. We have shown previously that acetone gives the same chemical shift variations as an ester bond,[1] so that the fatty acid's ester bonds could be safely modelled by acetone. The phosphodiester $(CH_3O)_2PO_2^-$, non-esterified oxygen atom was used as a hydrogen-bond acceptor to model the non-ester phosphate oxygen atoms of the lipid polar head group. The ^{13}C isotropic chemical shift differences between cholesterol/acetone (or cholesterol/water) and pure cholesterol have already been calculated and discussed in detail previously.[1] Briefly, the hydrogen-bond effects of acetone and the water-acceptor model are quantitatively very similar, giving an upfield (−) and downfield (+) chemical shift pattern (+, −, −, −, +, −) for C1–C6. This pattern is different for a water-donor-type hydrogen-bond (−, −, +, −, −, +), which shows the dependence on the nature of the hydrogen-bonding (through hydrogen or oxygen cholesterol hydroxy group atoms). The carbon chemical shift variations between dimethyl phosphate/cholesterol and pure cholesterol are presented in Figure 6a. Because the dimethyl phosphate is hydrogen-bonded to the cholesterol hydroxy group through one of its non-ester oxygen atoms, the variation pattern is qualitatively similar to that of acetone (+, −, −, −, +, −). However, the variation amplitudes are about five times larger, which indicates a much stronger effect of the $(CH_3O)_2PO_2^-$ negative charge on the electron density of the first cholesterol ring.

Following the procedure described in the Experimental Section, we explored all the possible linear combinations of individual chemical shift variations for the three C3–O3 rotamer states [*gauche* (+), *gauche* (−), and *anti*] and the four hydrogen-bonding partners (acetone, dimethyl phosphate, water acceptor and water donor) by using 1% increments for C1–C6. The errors in the experimental chemical shift variations were 0.1 ppm for C1–C4 and C6 (to take into account experimental accuracy and the nonspecific solvent effects on chemical shifts) and 0.2 ppm for C5 (which gives a broader line of low intensity). Only 8.1×10^6 combinations out of a total of 10^{12} satisfied the two filtering criteria (maximum error and rmsd) and thus provided a good fit between the calculated and experimental chemical shifts. The distributions of the seven coefficients are presented in Figure 7 and their averages (Table 2) were used to calculate the theoretical chemical shift variation pattern plotted in Figure 6b.

Concerning the rotamer distributions (Figure 7a), note that the *gauche* (+) conformation is quite well defined (with a standard deviation of 4%). On the other hand, the *gauche*

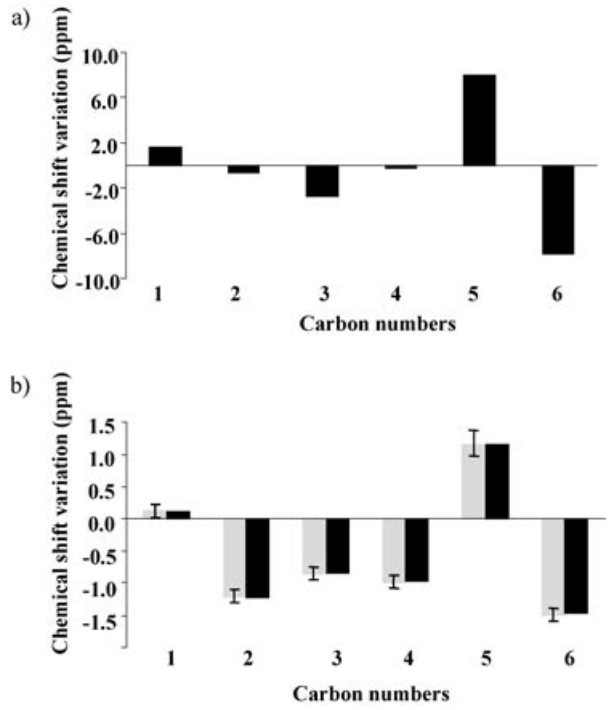

Figure 6. a) Theoretical chemical shift variations between phosphate/cholesterol and pure cholesterol. b) Experimental (grey) and theoretical (black) chemical shift variation patterns between cholesterol in membrane and in solution. The experimental error bars are 0.1 ppm for C1–C4 and C6 and 0.2 ppm for C5. The theoretical pattern was calculated for each carbon atom (C1–C6) by using Equation (3). The coefficients of the linear combinations for the rotamers (%j) and hydrogen-bonding partners (%k) correspond to the average values given in Table 2.

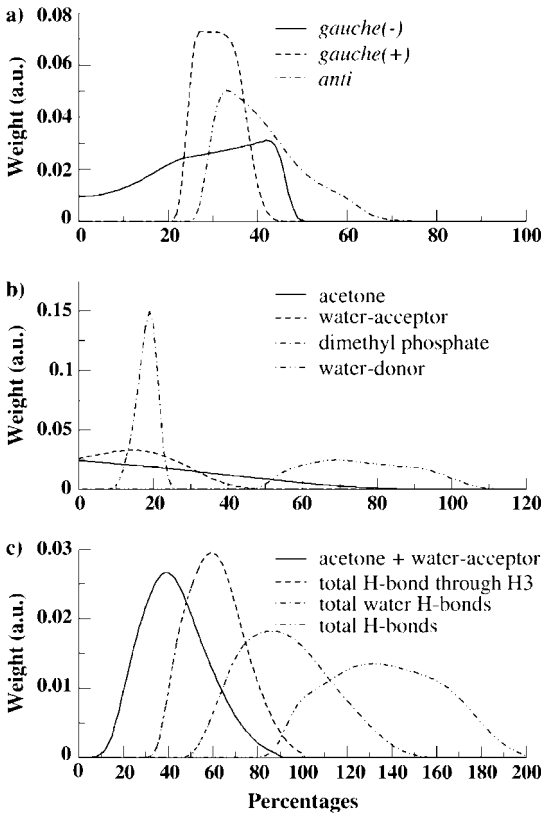

Figure 7. Distributions of the linear combination coefficients. The weight of each coefficient percentage is referenced to the total number of solutions. a) Rotameric conformer distributions. b) hydrogen-bonding partner distributions; c) distributions of the different types of hydrogen bonds.

Table 2. Average values and standard deviations of the rotameric states and hydrogen-bonding partner distributions.

Rotameric states	Average [%] ± standard deviation
gauche(−)	28 ± 12
gauche(+)	31 ± 4
anti	41 ± 9
hydrogen-bond partners	number of hydrogen bonds per cholesterol molecule [%][a]
through cholesterol H3	
acetone	26 ± 19
water acceptor	17 ± 10
dimethyl phosphate	18 ± 3
none	39 ± 13
through cholesterol O3	
water donor	76 ± 14
none	124 ± 14

[a] The number of hydrogen bonds per OH group was limited to one (or 100%) involving the hydrogen atom as a donor and two (or 200%) involving the oxygen atom as an acceptor (since the oxygen atom has two lone pairs). Since the fitting procedure only imposed a maximum value of hydrogen-bond partners, the final optimum result shows a certain percentage of OH groups free of hydrogen bonds, which is indicated as "none" in the table.

(−) and *anti* conformers have a larger distribution. However, it may be observed that an equal distribution of rotamers satisfies the experimental constraints and that the average values of our distribution are similar to these values (Table 2). It should be stressed that Figure 7a shows the distribution of coefficients for which a good agreement is found between the calculated and experimental data. However, it does not show the probability of the presence of each rotamer. Therefore, the dissymmetry in the distribution of the *anti* and *gauche* (−) rotamers may reflect a real tendency towards a higher content of *anti* rotamers as well as being merely due to the fact that our fitting problem is underdetermined.

Concerning the hydrogen-bonding partner distributions (Figure 7b and c), the major result that emerges from our statistical analysis is the very well-defined population of phosphodiester hydrogen-bonding (18 ± 3%). This can be explained by the large effect on the ^{13}C chemical shift produced by this chemical function (five-fold larger than acetone and water-acceptor groups). Consequently, a small variation of its corresponding percentage induces large chemical shift variations compared with cholesterol in solution. Two other chemical groups can interact with the hydroxy hydrogen atom, namely acetone (model for lipid esters) and a water acceptor. In contrast to dimethyl phosphate, their distribution is poorly defined with standard deviations of 19% and 10%, respectively, which represent more than 60% error on the average values. We know that hydrogen-bonding to these groups has similar effects on the cholesterol ^{13}C chemical shifts. Consequently, their distribution is difficult to determine separately with a good degree of accuracy.

However, if one considers the sum of these two contributions (acetone + water acceptor) for each set of parameters, one observes that the corresponding distribution is better defined, with a standard deviation of 30% of the average value ($43 \pm 14\%$). Our results show that less than one partner interacts with the hydrogen atom of the cholesterol's hydroxy group (total hydrogen-bond to H3 $= 61 \pm 13\%$). This indicates that within our theoretical approach, lipids do not always hydrogen-bond to cholesterol and that H3 can be free of any interaction, which may be due to the highly dynamic behavior of the cholesterol/DMPC system and its hydroxyl group.

The last interaction involves the hydroxy group's oxygen atom, which can only hydrogen-bond to water-donor-type neighbours. Its population is clearly larger than that of the water-acceptor-type molecule. This result differs from the molecular dynamics simulation analysis, which exhibits an inverse ratio.[12] However, our result is consistent with the fact that the oxygen atom has two hydrogen-bonding sites (i.e. two lone pairs), whereas the hydrogen atom can hydrogen-bond to only one partner. It is thus reasonable to conclude that the probability of interaction with the oxygen atom is larger than with the hydrogen atom. Furthermore, we know that the hydroxy group's hydrogen atom interacts with nonwater molecules. This reduces the probability of possible interactions with water acceptors and promotes the hydrogen-bonding ratio in favor of the oxygen atom of the hydroxy group. If one calculates the total number of hydrogen-bonded water molecules (Figure 7c), one obtains nearly one water molecule per cholesterol, which is close to the value obtained by molecular dynamics simulation (1.1 ± 0.1).[12] Finally, the total number of interactions (acetone, dimethyl phosphate and water) obtained by our theoretical and statistical analysis is equal to 1.4 per cholesterol molecule, which is again close to the value of 1.3 proposed by Pasenkiewicz-Gierula et al.[12]

The average values of the linear combination coefficient distributions have been used to calculate the theoretical chemical shift variations. These variations are plotted in Figure 6b and compared with the experimental ones. One can see very good concordance between these results, the linear fit between theoretical and experimental variation values gives a Pearson coefficient equal to 0.999 and a slope of 0.990.

However, note that there are a certain number of limitations to this approach. First, the accuracy of chemical shift variations is limited by the intrinsic low resolution of solid-state NMR spectra and by nonspecific solvent effects. For proton chemical shifts this was a major limitation since the variations observed upon hydrogen bonding were not much larger then the experimental accuracy, which is why this available information was not used in the analysis. Another limitation is related to the intrinsic accuracy of quantum-chemical calculations of chemical shifts. This problem was minimized by considering not the absolute chemical shifts but rather the variations induced by specific interactions. The validity of this treatment was established in our previous work.[1] The last limitation we want to mention arises from the fact that we fitted our data with a limited set of well-defined rigid structures, which were supposed to reflect the experimental situation. Of course the real system is much more complex and dynamic than is modeled here. Each hydrogen-bond effect should take into account the averaging of the internal dynamics of this bond. Other less significant hydrogen-bonding partners could have been included. This may affect the results and, in particular, the quantification of rotamers and hydrogen-bond distribution may be slightly modified.

Conclusions

In the work described herein, we first established a strategy to perform the complete proton and carbon assignment of cholesterol resonances in the membrane state without any use of the known solution-state assignment. This strategy largely relies on recently developed solid-state 2D NMR experiments and on the specific dynamics of cholesterol in fluid membranes, which prevents extensive spin diffusion and allows the *a priori* knowledge of H–C dipolar couplings to be used. We observed that the carbon chemical shifts of C1–C6 significantly deviate from their solution values. These deviations could be interpreted in terms of the C3–O3 rotameric distribution and the nature of the hydrogen-bonding partners of the cholesterol's hydroxy group. This could be achieved by calculating the chemical shifts using quantum-chemical methods, and because the effects of the various interactions with the hydroxy group have been validated previously by solution-state NMR experiments.[1] A useful extension of the ab initio calculations would be to analyze the chemical shifts in terms of localized bonding to describe more precisely the contributions of specific orbitals. This can be achieved by Natural Bond Order based Natural Chemical Shift analyses[57] and we are currently exploring this route.

Thus, we have directly demonstrated for the first time the interaction of the cholesterol's OH proton with the phosphatidylcholine's phosphodiester group, and quantified the percentage of such an interaction in the membrane state ($18 \pm 3\%$). The presence of other hydrogen-bonding partners has also been demonstrated, although their interactions have been quantified less accurately. Finally, we found no convincing evidence for the rotamer distribution of the OH group being very different from what it is in solution, that is, an equal population of the three major rotamers. As a result of this work it is now possible to perform a whole series of experiments using different lipid mixtures (saturated and polyunsaturated chains, sphingomyelin, phosphatidylethanolamine, phosphatidylserine, phosphatidic acid, glycolipids) and experimental conditions (temperature, hydration, osmotic pressure) which would allow the role of hydrogen bonds in specific sterol–lipid interactions to be specified.

Experimental Section

Samples: A sample of multilamellar vesicles (MLV) consisting of chain-deuteriated [D_{54}]DMPC (Avanti Polar Lipids, Alabaster, AL) and choles-

terol-^{13}C4,^{13}C3 (Cambridge Isotope Laboratories, Andover, MA) were prepared with 30 mol% of cholesterol (4 mg). The multilamellar vesicles were made by hydrating a film of a dry DMPC/Cholesterol mixture. After lyophilization the lipids were hydrated in the NMR rotor by addition of the same weight amount of D_2O. ^{2}H NMR spectroscopy (of a separate sample hydrated with deuterium-depleted H_2O) was used to check that the chain lipid quadrupolar splittings had standard values for such an MLV sample.

NMR experiments: The NMR experiments were performed on a Bruker DMX narrow bore spectrometer operating at a ^{1}H Larmor frequency of 500.13 MHz. All experiments were carried out at a sample temperature of 313 ± 2 K. To compensate for temperature increases in the rotor due to MAS, the driving air was precooled to a temperature that would give the desired temperature in the rotor. The known temperature dependence of the water chemical shift was used to check the temperature. Desiccation of the sample during the experiment was not observed. HSQC spectra were acquired using a 4 mm Bruker HR-MAS gradient probe. The MAS spinning rate was adjusted to $15 \text{ kHz} \pm 1$ Hz.[43] A conventional echo-antiecho gradient HSQC experiment, using a double INEPT polarization transfer, was used to obtain the ^{1}H–^{13}C correlations. Two 800 µs sine-shaped gradient pulses of 40 and 10.05 G cm^{-1} strength were used in the experiment to detect only the protons attached to a ^{13}C nucleus. The RF pulses were applied at B1-field strengths of 30.5 kHz for carbon and 39 kHz for proton, which corresponds to pulse widths of 8.2 and 6.4 µs, respectively. A total of 1024 increments (dwell time 20 µs), each with 32 scans were collected.

Dipolar HETCOR spectra were obtained with a 5 mm DOTY scientific XC-5 MAS probe at a spinning rate of 9 kHz. CP contact times were set to 2.5, 0.8, or 0.25 ms. A total of 128 $t1$ increments with a 50 µs dwell time and 512 scans each were recorded for all experiments. The ^{1}H-decoupling field was 66 kHz, and a TPPM decoupling scheme was employed during the acquisition time.[57]

Calculation of NMR chemical shift variation patterns: All NMR chemical shifts were calculated as described in the preceding publication.[1] Briefly, a Hartree–Fock strategy was used to determine the chemical shifts. Geometries were fully optimized at the HF/STO-3G level and isotropic chemical shifts were determined for all atoms at the same theoretical level using a double-zeta-type basis set with a polarization function [namely 6-31G(d,p)]. As shown previously, a two-ring molecular model could be used instead of performing calculations on the whole cholesterol molecule.

Supramolecular models, which combine the three major (C2, C3, O3, H) rotamer states [*gauche* (+), *gauche* (−), and *anti*, denoted as $g+$, $g-$, and *anti*, respectively] and the hydrogen-bonding partners of the hydroxy group of cholesterol, were separately calculated. We calculated the carbon chemical shift difference between each structure [$\delta_i^{theo}(j,k)$] and the average over the three rotamers of pure cholesterol [$\delta_i^{\text{theo}}(gaz)$, where j indicates the rotamer conformation, k the type of hydrogen-bonding partner, and $\delta^{\text{theo}}(gaz)$ is the chemical shift of the isolated molecule without hydrogen-bonding partners. This difference reflects the theoretical effect of a specific hydrogen-bonding interaction and the conformation of cholesterol in the "membrane" compared with cholesterol in "solution". For each carbon i, linear combinations of these chemical shift variations ($\Delta\delta_i^{\text{theo}}$) were compared with the experimental variations($\Delta\delta_i^{\text{exp}}$)[Eq. (1) and Eq. (2)].

$$\Delta\delta_i^{\text{theo}} = \sum_{j=g+,g-,anti} \%j \sum_{k=\text{H-bond partners}} \%k[\delta_i^{\text{theo}}(j,k) - \delta_i^{theo}(gaz)] \quad (1)$$

$$\Delta\delta_i^{\text{exp}} = [\delta_i^{\text{exp}}(\text{membrane}) - \delta_i^{\text{theo}}(CCl_4)] \quad (2)$$

The coefficients ($\%j$, $\%k$) of the linear combinations were varied by increments of 1% over all the rotameric states and all the hydrogen-bonding partners. It was necessary to verify for each coefficient set that $\sum_{j=g+,g-,anti} \%j = 100\%$ and $\sum_{k=\text{H-bond partners}} \%k \leq 300\%$, which corresponds to a maximum of three simultaneous hydrogen-bonding possibilities of cholesterol's hydroxy group (one to H3 and two to the O3 lone pairs).

The results were then filtered according to two criteria: 1) for each carbon, the difference between the experimental and theoretical variations must be lower than the corresponding experimental error ($|\Delta\delta_i^{\text{exp}} - \Delta\delta_i^{\text{theo}}| \leq \text{Err}_i^{\text{theo}}$); 2) the root mean square deviation (rmsd) must be lower than the average of all the carbon experimental errors [Eq. (3), where n = the number of carbon atoms].

$$\left(\sqrt{\sum_{i=1}^{n} \frac{(\Delta\delta_i^{\text{exp}} - \Delta\delta_i^{\text{theo}})^2}{n}} \leq \frac{\sum_{i=1}^{n} \text{Err}_i^{\text{exp}}}{n}\right) \quad (3)$$

Acknowledgements

The 500 MHz NMR spectrometer was financed by the CNRS (programme IMABIO) and the région Midi-Pyrénées. Bruker is acknowledged for carrying out the HR-MAS-HSQC experiment.

[1] F. Jolibois, O. Soubias, V. Réat, A. Milon, *Chem. Eur. J.* **2004**, *10*, preceding paper in this issue: DOI: 10.1002/chem.200400245.
[2] M. Y. el-Sayed, T. A. Guion, M. D. Fayer, *Biochemistry* **1986**, *25*, 4825.
[3] T. P. W. McMullen, R. N. McElhaney, *Curr. Opin. Colloid Interface Sci.* **1996**, *1*, 83.
[4] H. Ohvo-Rekila, B. Ramstedt, P. Leppimaki, J. P. Slotte, *Prog. Lipid Res.* **2002**, *41*, 66.
[5] P. A. Hyslop, B. Morel, R. D. Sauerheber, *Biochemistry* **1990**, *29*, 1025.
[6] T. Rog, M. Pasenkiewicz-Gierula, *Biophys. Chem.* **2004**, *107*, 151.
[7] F. T. Presti, R. J. Pace, S. I. Chan, *Biochemistry* **1982**, *21*, 3831.
[8] J. M. Boggs, *Biochim. Biophys. Acta* **1987**, *906*, 353.
[9] P. T. Wong, S. E. Capes, H. H. Mantsch, *Biochim. Biophys. Acta* **1989**, *980*, 37.
[10] R. Bittman, C. R. Kasireddy, P. Mattjus, J. P. Slotte, *Biochemistry* **1994**, *33*, 11 776.
[11] A. J. Robinson, W. G. Richards, P. J. Thomas, M. M. Hann, *Biophys. J.* **1995**, *68*, 164.
[12] M. Pasenkiewicz-Gierula, T. Rog, K. Kitamura, A. Kusumi, *Biophys. J.* **2000**, *78*, 1376.
[13] A. M. Smondyrev, M. L. Berkowitz, *Biophys. J.* **2001**, *80*, 1649.
[14] H. L. Scott, *Curr. Opin. Struct. Biol.* **2002**, *12*, 495.
[15] S. W. Chiu, E. Jakobsson, R. J. Mashl, H. L. Scott, *Biophys. J.* **2002**, *83*, 1842.
[16] N. P. Franks, W. R. Lieb, *J Mol. Biol.* **1979**, *133*, 469.
[17] C. H. Huang, *Lipids* **1977**, *12*, 348.
[18] A. Leonard, C. Escrive, M. Laguerre, E. Pebay-Peyroula, W. Neri, T. Pott, J. Katsaras, E. J. Dufourc, *Langmuir* **2001**, *17*, 2019.
[19] H. L. Scott, *Biophys. J.* **1991**, *59*, 445.
[20] M. Pasenkiewicz-Gierula, Y. Takaoka, H. Miyagawa, K. Kitamura, A. Kusumi, *J Phys Chem. A* **1997**, *101*, 3677.
[21] K. Tu, M. L. Klein, D. J. Tobias, *Biophys. J.* **1998**, *75*, 2147.
[22] A. M. Smondyrev, M. L. Berkowitz, *Biophys. J.* **1999**, *77*, 2075.
[23] E. Bicknell-Brown, K. G. Brown, *Biochem. Biophys. Res. Commun.* **1980**, *94*, 638.
[24] S. F. Bush, R. G. Adams, I. W. Levin, *Biochemistry* **1980**, *19*, 4429.
[25] R. Bittman, S. Clejan, S. Lund-Katz, M. C. Phillips, *Biochim. Biophys. Acta* **1984**, *772*, 117.
[26] P. Mattjus, R. Bittman, J. P. Slotte, *Langmuir* **1996**, *12*, 1284.
[27] S. P. Verma, D. F. Hoelzl Wallach, *Biochim. Biophys. Acta* **1973**, *330*, 122.
[28] P. L. Yeagle, R. B. Marlin, *Biophys. Biochem. Res. Commun.* **1976**, *69*, 775.
[29] C. Karolis, H. G. L. Coster, T. C. Chilcott, K. D. Barrow, *Biochim. Biophys. Acta* **1998**, *1368*, 247, and references therein.
[30] G. W. Stockton, I. C. Smith, *Chem. Phys. Lipids* **1976**, *17*, 251.
[31] P. L. Yeagle, W. C. Hutton, C. Huang, R. B. Martin, *Biochemistry* **1977**, *16*, 4344.
[32] E. J. Dufourc, E. J. Parish, S. Chitrakorn, I. C. P. Smith, *Biochemistry* **1984**, *23*, 6062.
[33] J. A. Urbina, S. Pekerar, H. B. Le, J. Patterson, B. Montez, E. Oldfield, *Biochim. Biophys. Acta* **1995**, *1238*, 163.

[34] J. A. Urbina, E. Oldfield in *Solid state nuclear magnetic resonance spectroscopic approaches to the study of molecular organization of biological membranes*, (Ed.: P. I. Haris, D. Chapman), IOS Press, Amsterdam, **1998**, p. 113.
[35] M. P. Marsan, I. Muller, C. Ramos, F. Rodriguez, E. J. Dufourc, J. Czaplicki, A. Milon, *Biophys. J.* **1999**, *76*, 351.
[36] Z. R. Croasmun, R. M. K. Carlson, *Two-dimentional NMR spectroscopy: Applications for chemists and biochemists*, Wiley-VCH, New York, **1994**.
[37] K. Schmidt-Rohr, J. D. Mao, *J. Am. Chem. Soc.* **2002**, *124*, 13938.
[38] B. Montez, E. Oldfield, J. A. Urbina, S. Pekerar, C. Husted, J. Patterson, *Biochim. Biophys. Acta* **1993**, *1152*, 314.
[39] A. Lesage, S. Steuernagel, L. Emsley, *J. Am. Chem. Soc.* **1998**, *120*, 7095.
[40] E. De Vita, L. Frydman, *J. Magn. Reson.* **2001**, *148*, 327.
[41] A. Lesage, L. Emsley, *J. Magn. Reson.* **2001**, *148*, 449.
[42] J. D. Gross, P. R. Costa, J. P. Dubacq, D. E. Warschawski, P. N. Lirsac, P. F. Devaux, R. G. Griffin, *J Magn. Reson. B* **1995**, *106*, 187.
[43] O. Soubias, M. Piotto, O. Saurel, O. Assemat, V. Réat, A. Milon, *J. Magn. Reson.* **2003**, *165*, 303.
[44] A. Lesage, C. Auger, S. Caldarelli, L. Emsley, *J. Am. Chem. Soc.* **1997**, *119*, 7867.
[45] A. Lesage, D. Sakellariou, S. Steuernagel, L. Emsley, *J. Am. Chem. Soc.* **1998**, *120*, 13194.
[46] A. Lesage, M. Bardet, L. Emsley, *J. Am. Chem. Soc.* **1999**, *121*, 10987.
[47] K. Schmidt-Rohr, H. W. Spiess, *Multidimensionnal Solid State NMR and Polymers*, Academic Press, New York, **1994**.
[48] W. Kolodziejski, J. Klinowski, *Chem. Rev.* **2002**, *102*, 613.
[49] J. H. Davis, M. Auger, R. S. Hodges, *Biophys. J.* **1995**, *69*, 1917.
[50] M. Lee, W. I. Goldburg, *Phys. Rev.* **1965**, *140*, A1261.
[51] O. Soubias, V. Réat, O. Saurel, A. Milon, *J. Magn. Reson.* **2002**, *158*, 143.
[52] R. Bittman, *Cholesterol: Its Functions and Metabolism in Biology and Medicine*, Plenum Press, New York (USA), **1997**.
[53] C. Le Guerneve, M. Auger, *Biophys. J.* **1995**, *68*, 1952.
[54] S. Bhattacharya, S. Haldar, *Biochim. Biophys. Acta* **2000**, *1467*, 39.
[55] A. Milon, O. Soubias, V. Reat, unpublished results.
[56] J. A. Bohmann, F. Weinhold, T. C. Farrar, *J. Chem. Phys.* **1997**, *107*, 1173.
[57] A. E. Bennet, C. E. Riensta, M. Auger, K. V. Lakshmi, R. G. Griffin, *J. Chem. Phys.* **1995**, *103*, 6951.

Received: March 15, 2004
Revised: July 13, 2004
Published online: October 21, 2004